Precise determination of the molecular geometry in fullerene C_{60} powder: A study of the structure factor by neutron scattering in a large momentum-transfer range

F. Leclercq, P. Damay, and M. Foukani
Lasir-CNRS, Hautes Etudes Industrielles, 13 rue de Toul, F-59046 Lille, France

P. Chieux
Institut Laue-Langevin 156X, F-38042 Grenoble, France

M. C. Bellissent-Funel
Laboratoire Léon Brillouin, CEA-CNRS, CE Saclay, F-91191 Gif-sur-Yvette CEDEX, France

A. Rassat and C. Fabre
Laboratoire de Chimie, CNRS, Ecole Normal Supérieure, 24 rue Lhomond, F-75231 Paris CEDEX 05, France
(Received 14 December 1992; revised manuscript received 18 February 1993)

The molecular structure of fullerene C_{60} has been determined with high precision using neutron scattering over a large range of momentum-transfer values. In the high-temperature plastic phase, at 295 K, the description of the complete structure factor in the 0–20-$Å^{-1}$ range, including Bragg and diffuse intensities, confirms the free reorientation of the C_{60} spherical molecules. This analysis gives the carbon-carbon bond length within the five-member ring (single bond) equal to 1.4527(7) Å, and that connecting five-member rings (double bond) equal to 1.3909(10) Å. As the temperature is lowered to 4 K, the structural parameters are extracted from the analysis of the intramolecular contributions to the diffuse intensity in the 6.5–20-$Å^{-1}$ range: the single bond is elongated [1.460(2) Å] and the double bond shortened [1.381(3) Å], indicating that electrons get more localized on the π orbitals. The calculation method allows us to consider small distortions from the ideal truncated icosahedral model (oblate or prolate deformations); the method could easily be extended to the study of substituted fullerene molecules.

I. INTRODUCTION

Since Krätschmer, Fostiropoulos, and Huffman[1] discovered a way to prepare large quantities of fullerene C_{60}, many physical and chemical properties of this unique compound have been investigated. Abundant literature has been devoted to the physical properties of C_{60} but we shall restrict ourselves to a summary of the results which are most relevant for our study of molecular geometry.[1–13]

The first clear indication that the C_{60} molecule had the shape of a truncated icosahedron probably came from Krätschmer, Fostiropoulos, and Huffman,[1] who showed that the IR spectrum agreed with the prediction of Coulombeau and Rassat[2] for this configuration. Results on ^{13}C NMR,[3] quasielastic neutron scattering, and, of course, structural investigations[4–10] confirmed that all carbon atoms were equivalent and formed pentagon rings linked by double bonds, in conformity with icosahedral symmetry.

With the truncated icosahedral model, a major point was then to determine the two bond lengths d_{C-C}, named p (for pentagon), and $d_{C=C}$ named h (for hexagon). Yannoni *et al.*[11] showed, from their NMR study of the ^{13}C-^{13}C magnetic dipolar coupling, that the two bond lengths were not equal, the difference being at least 0.04 Å. A first theoretical prediction[12] suggested $p=d_{C-C}=1.436$ Å and $h=d_{C=C}=1.418$ Å; a more recent calculation[13] gave 1.445 and 1.405 Å, respectively.

The bond lengths in free molecules of C_{60} have been measured directly at 700 °C by Hedberg *et al.*[4] using gas-phase electron diffraction and found to be $p=1.455(6)$ Å and $h=1.398(10)$ Å.

As far as the solid-state structure is concerned, interest is focused on both detailed intramolecular configuration and molecular arrangements as a function of temperature.[6–8] Molecules of C_{60} crystallize in a cubic close-packing arrangement. Above 260 K, the spherical C_{60} molecules are reorienting extremely rapidly, and the orientational disorder is compatible with the $Fm3m$ group. A refinement of the Bragg intensities at room temperature indicates that the scattering may be modeled by spherical shell of carbon atoms, but it does not allow a determination of the actual arrangement of the atoms on the sphere.[6–8] As reported by David and co-workers,[7] below 260 K a continuous frozen in of the reorientational motion is observed, ending around 86 K in an orientational glass. It is now admitted that, at low temperature, the compound crystallizes in the group $Pa3$, a variant of the $Fm3$ group, the molecules being oriented in such a way that a pentagon of one C_{60} molecule nearly faces a double bond of a hexagon of the neighboring molecule. In spite of the remaining static disorder, it has been possible to find different values of h and p when averaging over

 ©1993 The American Physical Society

the two sets of C-C distances given by the Rietveld analysis of the 5-K diffraction pattern, $h=1.391(20)$ Å and $p=1.455(12)$ Å.[7] More recently, the refinement of a model allowing two different orientations for the C_{60} molecules at 110 K gives $h=1.399(7)$ Å and $p=1.445(5)$ Å.[8]

Two different studies based on an analysis of the atomic radial distribution function[9,10] (RDF) readily obtained an average value of the bond length at 1.42 Å, but the width of the peaks in the real space does not allow a separation of the two bond lengths. From a fit of the three first peaks of the RDF, Li *et al.*[9] found $p=1.46$ Å and $h=1.39$ Å at 300 K. From a reverse Monte Carlo simulation of the molecular structure factor, assuming the truncated icosahedral geometry, Soper *et al.*[10] showed that the two bond lengths were not equal. These authors treated the difference $h-p$ as a perturbation to an ideal structure where $h=p$ and found $p=1.44$ Å and $h=1.40$ Å at 295 K with a precision of the order of 0.01 Å, and no significant temperature effect down to 20 K.

Beyond the structural aspect, there exists a more fundamental interest to measure bond lengths with a better accuracy. In molecular compounds such as fullerenes, which accommodate single and double bonds, the electronic structure and bond lengths are intimately related. If π orbitals were delocalized as in graphite or benzene, all bonds would have equal length (and the molecule could not exist because it ought to be flat); on the other hand, a difference $p-h\approx 0.04$ Å indicates that localization of the electrons on the double bonds is far from complete. The effect of electron localization on cluster interactions has recently been pointed out by Ashcroft.[14]

The aim of the present study is to determine with high accuracy the structure of the fullerene C_{60} molecule, in the solid state, from an analysis of the diffuse scattering measured in a large range of momentum transfer Q, with $Q=(4\pi/\lambda)\sin(\theta)$, 2θ being the scattering angle. As a difference from x-ray scattering form factors, the neutron-scattering lengths of atoms do not depend on the scattering angle; it is thus possible, using a short wavelength and large angles,[17] to determine the intramolecular distances of rigid molecules with an accuracy of the order of 10^{-3} Å, i.e., an improvement of an order of magnitude as compared to conventional scattering techniques. It is worth mentioning that considerable and recent progress in neutron-scattering instrumentation and data analysis (the various corrections being well documented in the case of nuclear reactor experiment[15–17]) has played a significant role in this work.

Sample preparation and experimental setup are given in Sec. II.

The formalism used to elucidate the experimental diffraction pattern displayed by molecular crystals in terms of crystalline ordering (Bragg peaks) and orientational disorder (diffuse intensity) including a brief mention of inelasticity corrections is reported in Sec. III.

In Sec. IV, the handling of data corrections is introduced and the equation used in the fitting procedure is defined as follows: (i) To include as much as possible the corrections as adjustable parameters. Indeed, it has been shown[17] that *a priori* inelastic or recoil corrections were not sufficiently precise to describe the falling off of the scattering intensity at large Q. (ii) To perform all calculations in Q space, avoiding termination errors due to Fourier transforming.

The results are reported and discussed in Sec. V. Details are given on a modelization of the Debye-Waller factors. The molecular parameters obtained at three temperatures and two wavelengths are presented with a discussion on the temperature dependence of electron localization. A modelization of the complete structure factor including Bragg and diffuse intensities in the plastic phase (295 K) is treated in detail. Finally, the possibility of determining the impurity content from an analysis of the residue of the fit is investigated.

A critical discussion of the declared precision is made in Sec. VI.

II. SAMPLE PREPARATION AND EXPERIMENTAL SETUP

A crude sample of soot has been prepared using the recipe described by Haufler *et al.*[18] Purification was carried out following Allemand *et al.*[19] High-pressure liquid chromatography, IR, UV, and mass spectroscopy analysis did not reveal significant impurity. The compound was heated overnight under vacuum at 440 K, washed with deuterated benzene and heated again under vacuum for 12 h. As will be seen in Sec. IV, our study did not detect any residual solvent in the product.

The experiment was performed on the diffractometer 7C2 at the Orphée Reactor (Laboratoire Léon Brillouin) in Saclay. The spectrometer is equipped with a 640 BF_3 cells multidetector. The angular step between two adjacent cells is 0.2°; thus, the maximum diffraction angle is 128° if the first cell is located at the incident beam. Two wavelengths were used, $\lambda_1\approx 0.55$ Å and $\lambda_2=0.70$ Å, which allow maximum values of the vector transfer equal to 19.8 and 16.0 $Å^{-1}$, respectively.

The two wavelengths were calibrated at $\lambda_1=0.5684(8)$ Å and $\lambda_2=0.7058(13)$ Å with nickel powder. This calibration based on a linear fit of the ten main Bragg peak positions (assuming Gaussian peak shape) also gave the zero-angle offset and provided an experimental check of the diffractometer resolution function up to $Q=12$ $Å^{-1}$.

The 1.5-g C_{60} sample was contained in a tight cylindrical vanadium cell (5-mm inner diameter, 0.1-mm thick, and 50-mm high). The experiment was carried out at three temperatures 4, 150, and 295 K in a dedicated Institut Laue Langevin-type cryostat equipped with a vanadium tail, in order to study the three phases described by David *et al.*[7] The data handling, in particular corrections for the container, self-absorption, and multiscattering, were performed using the conventional procedure.[20]

III. FORMALISM

The aim of this section is to present the formalism used to describe in a unified way the static structure factor $S(\mathbf{Q})$ of molecular crystals presenting an orientational (static and/or dynamic) disorder, according to Dolling, Powell, and Sears.[21] Molecules arranged on an ordered lattice give rise to coherent elastic intensity located at Bragg positions, the corresponding structure factor being

called $S_c(\mathbf{Q})$; in addition the orientational disorder, characterized by fluctuations around the molecular average conformation and orientation, produces, over the whole Q range, diffuse scattering noted $S_d(\mathbf{Q})$.

The static structure factor $S(\mathbf{Q})=S_c(\mathbf{Q})+S_d(\mathbf{Q})$ is obtained by summing up the dynamical structure factor $S(\mathbf{Q},\omega)$ over all energy transfers $\omega=\varepsilon_0-\varepsilon=(\hbar/2m)(k_0^2-k^2)$. Then,

$$S(\mathbf{Q})=\int_{-\infty}^{+\infty} S(\mathbf{Q}(\omega),\omega)d\omega \tag{1}$$

with $\mathbf{k}_0$ and $\mathbf{k}$, the initial and final values of the wave vectors

$$\mathbf{Q}(\omega)=\mathbf{k}_0-\mathbf{k} .$$

$\mathbf{Q}=\mathbf{Q}(0)$, the modulus of which being the elastic momentum transfer $Q=2k_0\sin\theta=(4\pi/\lambda)\sin\theta$, with 2θ the scattering angle.

In a conventional diffraction experiment, the intensity is measured as a function of the scattering angle 2θ for a fixed incident neutron energy $\hbar\varepsilon_0$, and the observed intensity is proportional to the differential scattering cross section per unit solid angle $d\Omega$,

$$\frac{d\sigma}{d\Omega}=\int_0^\infty \frac{d^2\sigma}{d\Omega\, d\varepsilon}d\varepsilon=\int_0^\infty \eta(\varepsilon)\frac{k}{k_0}S[\mathbf{Q}(\omega),\omega]d\varepsilon$$
$$=\eta(\varepsilon_0)S_c(\mathbf{Q})+\int_{-\infty}^{\varepsilon_0}\eta(\varepsilon_0-\omega)\left[1-\frac{\omega}{\varepsilon_0}\right]^{1/2}$$
$$\times S_d[\mathbf{Q}(\omega),\omega]d\omega , \tag{2}$$

where $\eta(\varepsilon)$ is the energy-dependent efficiency of the detector.

In the quasistatic approximation, the second term of this equation must be corrected for inelasticity, following Placzek,[22]

$$\frac{d\sigma}{d\Omega}=\eta(\varepsilon_0)[S_c(\mathbf{Q})+S_d(\mathbf{Q})+P(\mathbf{Q},\varepsilon_0)] , \tag{3}$$

where $P(\mathbf{Q},\varepsilon_0)$ may be expanded as a function of even powers of Q. This correcting term will be included in the data handling and will be dropped for simplicity in the following.

Let us now formulate the intramolecular and intermolecular contributions to the total diffraction pattern displayed by a molecular crystal. The differential scattering cross section of neutrons by an assembly of fixed nuclei is written as

$$\frac{d\sigma}{d\Omega}\propto\left\langle\sum_{i,j}b_i b_j^*\exp[i\mathbf{Q}\cdot(\mathbf{r}_i-\mathbf{r}_j)]\right\rangle , \tag{4}$$

where b_i is the scattering length, the angular brackets are for space and time average, and the summation is performed over all nuclei in the system.

In a molecular system and also to describe thermal and orientational disorder in a molecular crystal[21] it is convenient to express the position vector of the ith atom using the molecular center of mass as a reference,

$$\mathbf{r}_i=\mathbf{R}_m+\mathbf{r}_{mi} , \tag{5}$$

where $\mathbf{R}_m$ is the position vector of the center of mass of the mth molecule and $\mathbf{r}_{mi}$ is the position of the atom i relative to the center of mass.

The sum of the atomic contributions to the molecule m allows the definition of its molecular form factor F_m,

$$F_m=\sum_{i(m)} b_i\exp(i\mathbf{Q}\cdot\mathbf{r}_{mi}) . \tag{6}$$

Using Eq. (5) and after separating intramolecular ($m=m'$) and intermolecular ($m\neq m'$) components, Eq. (4) gives

$$\frac{d\sigma}{d\Omega}\propto\sum_m\langle F_m^2\rangle+\left\langle\sum_{m\neq m'}\exp[i\mathbf{Q}\cdot(\mathbf{R}_m-\mathbf{R}_{m'})]\sum_{i(m)}\sum_{j(m')}b_i b_j^*\exp[i\mathbf{Q}\cdot(\mathbf{r}_{mi}-\mathbf{r}_{m'j})]\right\rangle$$
$$=\sum_m\langle F_m^2\rangle+\sum_{m\neq m'}\exp[i\mathbf{Q}\cdot\langle\mathbf{R}_m-\mathbf{R}_{m'}\rangle]e^{-2W}\langle F_m F_{m'}^*\rangle , \tag{7}$$

where it is assumed that the fluctuation of one atom around its equilibrium position can be split in translational motion of the molecular center of mass and intramolecular rotations or vibrations. The Debye-Waller factor $W=\frac{1}{2}\langle\delta R_m^2\rangle Q^2$ is relative to the center of mass. The term $\langle F_m F_{m'}^*\rangle$ contains information on the intermolecular orientational correlations and their range.

For a system of N identical molecules with similar orientations or nearly spherical molecules (i.e., no preferential orientation) and neglecting the correlation between orientational fluctuations of neighboring molecules, $\langle F_m F_{m'}^*\rangle_{m\neq m'}=\langle F\rangle^2$ and Eq. (7) simplify to

$$\frac{d\sigma}{d\Omega}\propto\left\{\sum_{m,m'}\langle F\rangle^2 e^{-i\mathbf{Q}\cdot\langle\mathbf{R}_m-\mathbf{R}_{m'}\rangle}e^{-2W}\right.$$
$$\left.+N[\langle F^2\rangle-\langle F\rangle^2 e^{-2W}]\right\}=S_c(\mathbf{Q})+S_d(\mathbf{Q}) . \tag{8}$$

In a molecular crystal, the first term $S_c(\mathbf{Q})$ gives rise to sharp Bragg peaks due to molecular ordering on the crystal sites and the diffuse scattering term can be developed as follows:

$$S_d(\mathbf{Q})=N[\langle F^2\rangle-\langle F\rangle^2 e^{-2W}]$$
$$=N\{(\Delta F)^2+\langle F\rangle^2(1-e^{-2W})\} , \tag{9}$$

where $(\Delta F)^2=\langle F^2\rangle-\langle F\rangle^2$ takes into account the average orientational and conformational disorder of the molecules and $\langle F\rangle^2(1-e^{-2W})$ is due to thermal fluctuations of the molecular center of mass.

At large-Q values, the leading term in Eq. (8) is the "molecular structure factor" $N\langle F^2\rangle$ since the $\langle F\rangle^2 e^{-2W}$ contribution is strongly damped leading to a vanishing Bragg intensity (in molecular crystals, there are generally no more Bragg peaks visible at momentum transfers Q larger than 10 Å^{-1}). In this limit, only intramolecular

bonds contribute to the diffraction pattern and Eq. (8) reduces to

$$\langle F^2\rangle = \sum_{i(m),j(m)} \overline{b_i b_j^*}\langle \exp[i\mathbf{Q}\cdot(\mathbf{r}_{mi}-\mathbf{r}_{mj})]\rangle = \sum_{i,j(m)} \overline{b_i}\,\overline{b_j}\frac{\sin(Qr_{ij})}{Qr_{ij}}\exp\left[\frac{-\langle \delta r_{ij}^2\rangle Q^2}{2}\right] + \sum_{i(m)}\frac{\sigma_i}{4\pi} . \tag{10}$$

The last expression of this equation is obtained after averaging over all possible orientations of $\mathbf{r}_{ij}$, i.e., assuming an isotropic orientational disorder or performing a powder averaging on a crystalline sample, where $\overline{b_i}$ is the coherent scattering length and σ_i the incoherent cross section of the atom i, and the Debye-Waller factors $W_{ij}=\frac{1}{2}\langle \delta r_{ij}^2\rangle Q^2$ account for intramolecular vibrations in the harmonic approximation.[23] The molecular structure factor $\langle F^2\rangle$ may be split in the usual way into a distinct term $\langle F^2\rangle_{\rm dist}(i\neq j)$ and a self term $\langle F^2\rangle_{\rm self}(i=j)$.

IV. DATA ANALYSIS AND FITTING PROCEDURE

Several corrections must be performed on the raw data before fitting. The usual corrections for container scattering, sample attentuation, and multiple scattering were made using the results of additional experiments done on the empty container, vanadium bar, and empty cryostat. The inelasticity and recoil corrections were included into the fitting equation, a procedure that proved to be more accurate:[17] indeed if a theoretical formulation of these corrections is known, their calculation *ab initio* supposes hypothesis to evaluate the effective mass of the scattering atoms in the molecular entities; moreover, the fit of the correction parameters allows to take into account cross terms from multiple scattering and inelasticity.

A. Inelasticity correction

Following Eq. (3), Placzek's[22] correction must be applied on the self part ($i=j$) of the molecular structure factor [Eq. (10)] and may be developed as a series expansion of $Q^2, Q^4, Q^6, \ldots$,

$$\langle F^2\rangle_{\rm self,corr} = \langle F^2\rangle_{\rm self,meas} \times \left[1 - A\frac{m_n}{M_{\rm eff}}\left[\frac{\lambda}{4\pi}\right]^2 Q^2 + \cdots\right], \tag{11}$$

where A is a constant characteristic of the wavelength dependence of the detector efficiency, m_n is the neutron mass, and $M_{\rm eff}$ is an effective mass for the system. Instead of evaluating the correction *a priori*, we chose to add in the fit a function $1+A_1Q^2+A_2Q^4+A_3Q^6$ with three adjustable parameters. The effect of the coefficient A_3 is small and plays a role only above 20 Å^{-1}.

B. Recoil correction

For light atoms (or molecules), the distinct term [$i\neq j$, in Eq. (10)] must also be corrected for recoil in systems where the atoms (or molecules) are allowed to move more or less freely. The effect of this correction leads to a rescaling of the momentum-transfer scale. If $Q_{\rm eff}$ is the recoil corrected momentum-transfer vector, one may write, following Walford, Clarke, and Dore[24] from simple billiard ball mechanics,

$$\left[\frac{Q_{\rm eff}}{Q}\right]^2 = \frac{1+C_E^2(\theta)-2C_E(\theta)\cos 2\theta}{2(1-\cos 2\theta)} \tag{12}$$

with

$$C_E(\theta)=\frac{m_n}{m_n+M}\left\{\cos 2\theta + \left[\left[\frac{M}{m_n}\right]^2-\sin^2 2\theta\right]^{1/2}\right\} .$$

The correction depends on the ratio M/m_n, where M is the mass of the scatterer and m_n the neutron mass. For a rigid crystal, M goes to infinity while in a gas M is the molecular mass. In a plastic crystal, M is an effective mass since the molecules are neither free to move nor tightly bonded to the lattice; this unknown effective mass is also determined from the fit.

For M/m_n equal or larger than 20, a first-order expansion of Eq. (12) is sufficient,

$$Q_{\rm eff}=Q\left[1-\frac{m_n}{M}\left[\frac{\lambda}{4\pi}\right]^2 Q^2\right] . \tag{13}$$

C. Fitting equation

At large Q values, the molecular structure factor $\langle F^2\rangle$ is fitted using the following equation including inelasticity and recoil corrections,[25]

$$\langle F^2\rangle = A_0(1+A_1Q^2+A_2Q^4+A_3Q^6) + B\sum_{i\neq j(m)}\left[\overline{b_i}\,\overline{b_j}\frac{\sin(Q_{\rm eff}r_{ij})}{Q_{\rm eff}r_{ij}}\exp\left[\frac{-\langle \delta r_{ij}^2\rangle Q_{\rm eff}^2}{2}\right]\right], \tag{14}$$

where A_0 and B are normalization factors.

Large-Q neutron scattering is generally used to determine the structure of small rigid molecules. For a molecule containing n atoms, the number of free parameters used in Eq. (14) is equal to $6+n(n-1)$ and the computation gets out of hand for n exceeding 5 or 6. In the case of the fullerene C_{60}, the number of intramolecular distances is 1770; there would be no way to determine the molecular structure if it had not a very high symmetry. If the truncated icosahedron model is accepted, then all the atoms are equivalent (a gain of a factor 60), and the number of distinct intramolecular distances falls to 23. In such case, the number of free parameters is 52. Actually, it is known that only two bond lengths d_{C-C} and $d_{C=C}$, that we call, respectively, p and h, are sufficient to build the set of 23 distances $r_{ij}=f(h,p)$ (the calculation of the 23 intramolecular distances as a function of the independent parameters h and p has been included in the fitting program—see Ref. 25). Therefore the number of free parameters drops to 31, that is to say A_i, B, M, h, p, and 23 Debye-Waller factors.

We will show that an analysis of the Debye-Waller factors will allow us to model the δr_{ij}; as an example, if a

function such as $\langle \delta r_{ij}^2 \rangle = f(\langle \delta h^2 \rangle, \langle \delta p^2 \rangle)$ is found, the total number of free parameters drops to 10.

D. Low-Q cutoff for the fit

The total scattering pattern actually observed is the sum of Bragg intensity, diffuse scattering due to the translational and rotational motion of the whole molecule and a diffuse scattering due to the intramolecular contributions [Eq. (8)]. The relative weight of the molecular structure factor $\langle F^2 \rangle$ increases with Q. A delicate choice is to define above which value of Q Eq. (14) may be used safely. Moreover, since the precision of the final result depends on the breadth of the Q range investigated, it may be interesting to lower the $Q_{\min}$ value by removing the small Bragg peaks discernible in the intermediate range. At the three investigated temperatures, there are no Bragg peaks detectable for Q larger than 7 Å^{-1}; in the best case (295-K pattern), it has been possible to lower the cutoff down to 2.6 Å^{-1}.

V. RESULTS

The observed spectra at 4 and 295 K are reported in Figs. 1(a) and 1(b). We regroup here the presentation and the discussion around four topics: the study and modeli-

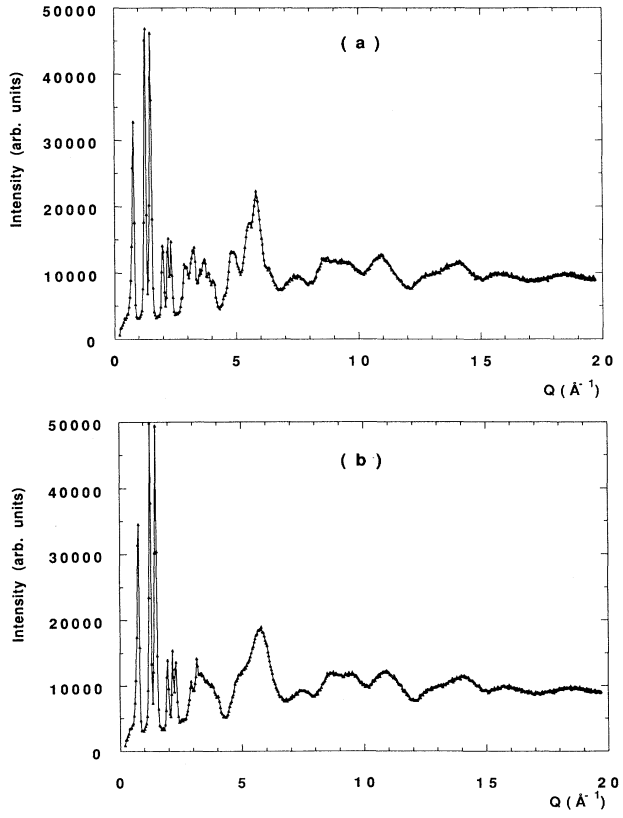

FIG. 1. Experimental diffraction patterns for the powder C_{60} sample for a 0.5684-Å wavelength at 4 K (a) and 295 K (b). Bragg peaks are visible in the low-Q range, $1 < Q < 6.5$ Å^{-1} at 4 K and $1 < Q < 3.5$ Å^{-1} at 295 K. The spectra are mainly governed by the molecular structure factor for Q values larger than 6.5 Å^{-1} at both temperatures.

zation of the Debye-Waller factors, the effect of temperature, a detailed investigation of the 295-K data in the whole Q range, and the sample purity.

A. Study of the Debye-Waller factors

The first concern was to reduce the number of free parameters by looking for correlations between the 23 Debye-Waller factors. Indeed, if the intramolecular distances are linear functions of h and p, their average fluctuations δr_{ij} and thus the Debye-Waller factors are surely not independent.

The 23 Debye-Waller factors obtained from a data fit using 31 independent parameters are reported in Fig. 2 as a function of the distance; the bond lengths h and p given by this fit are reported in Table I row *a*. The Debye-Waller factors obtained by Hedberg *et al.*[4] from the gas phase are also reported in Fig. 2 for comparison. It is striking that the Debye-Waller factors depend linearly on the interatomic distances. One obtains $\langle \delta r_{ij}^2 \rangle = 0.0029 r_{ij}$ from our data and $\langle \delta r_{ij}^2 \rangle = 0.00294 r_{ij}$ from the gas-phase data. This behavior is expected for a simple model in which h and p vibrate independently; strictly speaking, a linear relationship requires that $\langle \delta h^2 \rangle / h$ and $\langle \delta p^2 \rangle / p$ are of the same magnitude.

Several trials with 10 parameter fits involving a correlation between the h and p bond-length fluctuations (for example, $\delta h = \alpha \delta p$ or $\delta \rho = 0$, with ρ the radius of the sphere described by the carbon atoms) gave poor results, confirming the independence of the fluctuations δh and δp. Consequently, we used the general function

$$\langle \delta r_{ij}^2 \rangle = \frac{\partial r_{ij}}{\partial h} \langle \delta h^2 \rangle + \frac{\partial r_{ij}}{\partial p} \langle \delta p^2 \rangle \tag{15}$$

in order to reduce the Debye-Waller parameters from 23 to 2.

The values of $\langle \delta h^2 \rangle / h$ and $\langle \delta p^2 \rangle / p$ found from 295-K data in the 4–20-Å^{-1} Q range (Table I—fit *d*) are, respectively, 0.0031 and 0.0028 Å, values close enough to assure an almost linear dependence of $\langle \delta r_{ij}^2 \rangle$ with r_{ij}. The reduction of the number of free parameters from 31

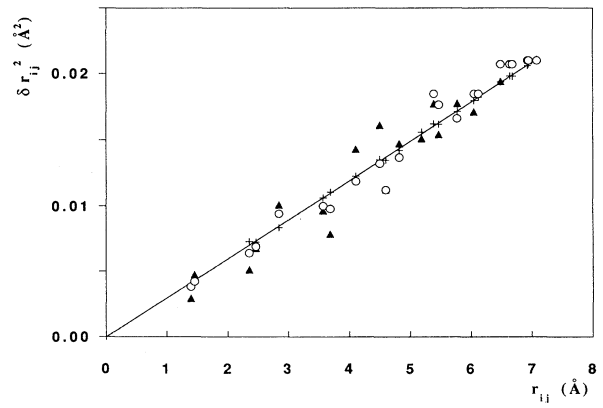

FIG. 2. Mean-square displacements δr_{ij}^2 as a function of interatomic distances r_{ij} [○, fitted values in this work; ▲, from Hedberg *et al.* (Ref. 4); and +, values calculated according to Eq. (15), assuming uncorrelated bond-length fluctuations].

to 10 did not significantly increase the residue; that guarantees the validity of this Debye-Waller factors model.

B. Temperature effect

The results of the fits for the three temperatures and two wavelengths are reported in Table I (rows *b* to *d*). The errors quoted in brackets correspond to one standard deviation. As an illustration of the quality of the fit, Fig. 3 reports experimental and calculated data at high temperature for a fit performed in the 2.6–20-Å^{-1} Q range, after filtering of the remaining Bragg intensity still visible in the 2.9 to 3.4-Å^{-1} Q values.

Let us first discuss the accuracy of the fit and the precision obtained on the values h and p. A $Q_{\min}$ cutoff of 6.5 Å^{-1} was chosen for the five runs; all data points were kept at 150 and 295 K while at 4 K several small Bragg peaks had to be removed in the 7.0–7.2- and 8.1–8.5-Å^{-1} Q ranges. At 295 K, results for a cutoff equal to 4 Å^{-1} are also reported. The precision on bond lengths is improved using $\lambda=0.70$ Å for which a better counting rate and statistics are obtained; but the estimation of the average fluctuations of bond lengths δr_{ij} is more precise with the short wavelength since the highest value of Q is extended from 16 to 20 Å^{-1}. Many trials have been made to check the effect of cutoff and filtering of the Bragg peaks. The greatest variation found for the value of h was 4×10^{-3} Å for cutoff values ranging from 2.6 to 11 Å^{-1}; for example h varies from 1.3906 Å 1.3933 Å for respective cutoff of 4 and 6.5 Å^{-1} (Table I–fits d'' and d'''). The stability of h and p is confirmed while examining the covariance matrix, which is reported in Table II. A correlation of the order of 0.05 is considered as negligible in least squares fitting but it is, in fact, rarely observed. One observes that parameters h and p are essentially coupled to each other; a weak coupling also exists between h and p and the recoil coefficient which is expected since the recoil correction changes the Q scale and therefore the length scale. But the recoil effective mass is so large (more than 700) that its effect is negligible and the effective mass was chosen as infinite in the final fits.

Considering now the temperature effect on the bond lengths h and p, which is shown in Fig. 4 using $\lambda=0.70$ Å and a cutoff at 6.5 Å^{-1}, one observes a significant increase of the double bond h between 4 and 150 K and a corresponding shortening of the single bond p. This effect corresponds to a localization of the electrons on the double bonds at low temperature.

Pauling[26] considered the effect of partial double bond character (bond number) on the bond length for a variety of compounds and proposed a simple model written as

$$n=\exp[c(L_n-L_1)]\ , \tag{16}$$

where n is the bond number ranging from 1 to 2, L_1 is the single bond length (1.541 Å for a C—C bond), L_n is the actual bond length depending on the partial double bond character, and the constant $c=-3.398$ is easily determined from $L_2=1.337$ Å for a C=C bond. However, absolute estimates of n using Eq. (16) are often not correct since bond lengths also depend on the molecular

TABLE I. Table I summarizes the main results of the data analysis, following the various approaches described in this work. The first column gives the label of the fit as referred in the text; the experimental conditions are quoted in columns 2 (wavelength) and 3 (temperature); the Q range investigated is reported in column 4; values of physical parameters returned by the fit are given in columns 5–9, respectively, $h=d_{C=C}$, $\langle\delta h\rangle$ being the fluctuation around the average h value, $p=d_{C-C}$, $\langle\delta p\rangle$, ρ the radius of the fullerene sphere; in columns 10 and 11 the bond numbers calculated according to Eq. (17) are given; finally, the residue of the fit and some comments are reported.

N^0	λ (Å)	T (K)	Q range (Å^{-1})	h (Å)	$\langle\delta h\rangle$ (Å)	p (Å)	$\langle\delta p\rangle$ (Å)	ρ (Å)	$n(h)$	$n(p)$	Residue (%)	Comments
a	0.5684(6)	295	4–20	1.391(5)		1.452(3)		3.544(6)			0.92	31 fitted parameters
b	0.5684(6)	4	6.5–20	1.3814(27)	0.061(3)	1.4597(18)	0.059(2)	3.547(4)	1.570	1.215	0.30	9 fitted parameters
b'	0.7058(13)	4	6.5–16	1.3827(17)	0.054(6)	1.4630(10)	0.063(8)	3.554(4)	1.576	1.212	0.31	(no recoil correction)
c	0.7058(13)	150	6.5–16	1.3928(10)	0.050(8)	1.4554(5)	0.066(8)	3.551(2)	1.522	1.239	0.50	
d	0.5684(6)	295	4–20	1.3894(21)	0.062(2)	1.4533(11)	0.068(2)	3.543(4)	1.526	1.237	0.93	
d'	0.5684(6)	295	6.5–20	1.3889(32)	0.062(4)	1.4541(17)	0.073(4)	3.544(6)	1.530	1.235	0.63	
d''	0.7058(13)	295	4–16	1.3906(10)	0.054(7)	1.4535(6)	0.071(7)	3.545(2)	1.523	1.238	0.47	
d'''	0.7058(13)	295	6.5–16	1.3933(18)	0.053(8)	1.4545(9)	0.070(8)	3.550(4)	1.518	1.241	0.20	
e	0.5684(6)	295	full range	**1.3909(10)**	**0.057(2)**	**1.4527(7)**	**0.067(2)**	3.545(2)	1.520	1.240	**0.57**	9 fitted parameters
e'	0.5684(6)	295	1.6–10	1.3905(30)	0.081(15)	1.4530(20)	0.044(14)				0.66	(no recoil correction)
e''	0.7058(13)	295	full range	**1.3913(22)**	**0.063(8)**	**1.4524(11)**	**0.066(6)**	3.544(4)	1.518	1.241	**0.68**	

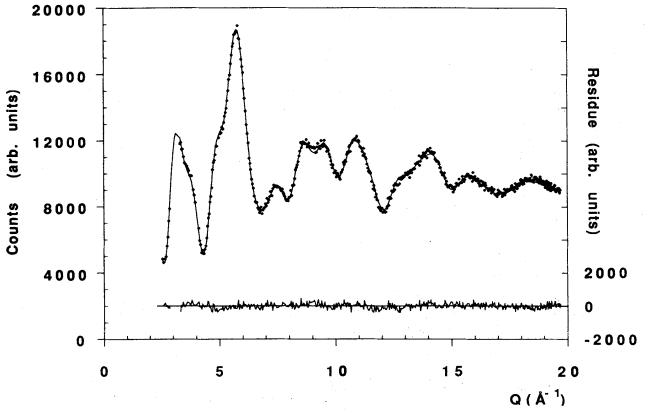

FIG. 3. Experimental (●) and calculated (——) diffraction pattern of fullerene powder obtained at 295 K with $\lambda=0.5684$ Å, after filtering of Bragg peaks. As can be seen on this double-y graph, the difference between calculated and experimental values as a function of Q is structureless.

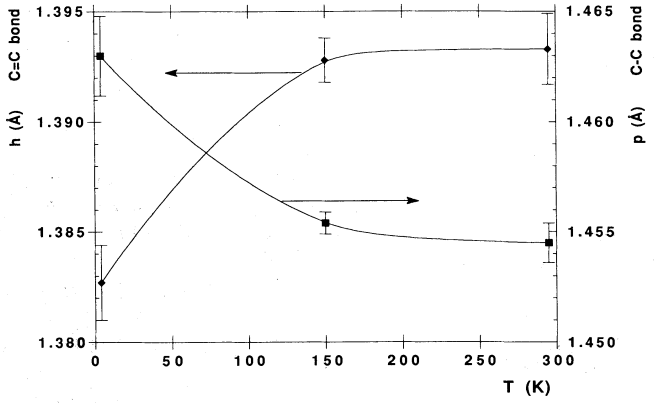

FIG. 4. Bond lengths $h=d_{C=C}$ (◆) and $p=d_{C-C}$ (■) as a function of temperature from an analysis of the data obtained at $\lambda=0.7058$ Å (fits b', c, and d'''). As the temperature is lowered from room temperature down to 4 K, the single bond is elongated ($\Delta h=+0.008$ Å) while the double bond is shortened ($\Delta h=-0.010$ Å); the electrons are more localized on the double bond at low temperature.

arrangement; for example the value $n=1.61$ found for benzene would correspond to 3.66 π orbitals instead of 3, but the prediction is correct for graphite. In the C_{60} molecule, the estimates are also incorrect since the calculated bond numbers correspond to 39 π orbitals instead of 30. Therefore, the values of bond numbers for C=C and C—C, reported in Table I—columns $n(h)$ and $n(p)$, respectively, have been calculated using a differential form of Eq. (16),

$$\frac{n_{h(\text{or}\,p)}-\bar{n}}{\bar{n}}=c[h(\text{or}\,p)-\bar{L}]\ , \tag{17}$$

where $\bar{n}=1.333$ is adjusted to accommodate 30 electrons equally delocalized on the 90 bonds, with an average bond length $\bar{L}(h+2p/3)$. With this approach it is possible to give a quantitative estimate of the localization of the electrons on the double bond as temperature is lowered from room temperature to 4 K; indeed, the h-bond number increases from 1.52 to 1.58 while the p-bond number decreases from 1.24 to 1.215. This localization occurs as an orientational ordering of the molecule is observed, increasing interactions with the neighboring molecules.

A last remark to be made is the very weak temperature effect on the radius ρ of the spherical shell of carbon atoms (see Table I). Taking, for example, fits performed in same Q range, one obtains, respectively, $\rho_{4\text{ K}}=3.554(4)$ Å (fit b'), $\rho_{150\text{ K}}=3.551(2)$ Å (fit c), and $\rho_{295\text{ K}}=3.550(4)$ Å (fit d'''), indicating that there is an almost complete compensation between h and p temperature effects, ending in an approximately constant value of the molecular radius over the whole temperature range (the slight contraction of ρ with increasing temperature is about 4.10^{-3} Å, i.e., of the order of the uncertainty).

C. Complete description of the Bragg and diffuse scattering at 295 K

It is now well confirmed that the fullerene C_{60} undergoes rapid isotropic reorientation above 260 K; the most convincing evidence is the narrowing of the ^{13}C NMR resonance line at room temperature reported by Yannoni *et al.*[11] The refinement of the crystalline structure,[6,7] as well as the quasielastic neutron-scattering measurements, is also consistent with rotations which are not correlated with the orientation of the neighboring molecules. In this ideal case, the average molecular form factor $\langle F\rangle$ reduces to

TABLE II. Covariance matrix of the 10-parameter fits as defined in Eq. (14).

	A_0	B	h	$\langle\delta h\rangle$	p	$\langle\delta p\rangle$	Recoil	A_1	A_2	A_3
A_0	1.000									
B	0.421	1.000								
h	−0.005	0.047	1.000							
$\langle\Delta h\rangle$	−0.044	0.099	0.023	1.000						
p	0.033	−0.054	−0.763	0.094	1.000					
$\langle\Delta p\rangle$	0.169	0.165	−0.062	−0.782	−0.015	1.000				
recoil	−0.012	−0.105	−0.153	−0.082	0.143	0.030	1.000			
A_1	−0.880	−0.332	−0.039	−0.067	−0.049	−0.178	0.074	1.000		
A_2	0.771	0.277	0.077	−0.076	−0.066	0.154	−0.119	−0.097	1.000	
A_3	−0.603	−0.241	−0.108	0.076	0.082	−0.133	0.150	0.087	−0.986	1.000

$$\langle F\rangle=\sum_{i(m)}\bar{b}_i j_0(Q\rho)\ , \tag{18}$$

where ρ is the radius of the sphere formed by the carbon atoms and $j_0(Q\rho)$ is the spherical Bessell function. A complete refinement of the structure factor $S(Q)$ at room temperature including Bragg intensities and diffuse scattering may thus be determined using Eq. (8). The calculation is carried out in steps: (i) The refinement of the most intense Bragg peaks, with the help of Eq. (18), is made first; (ii) a realistic diffraction pattern is then constructed for more than 100 peaks convoluted with the spectrometer resolution; and (iii) this pattern is subtracted from the total spectrum and the diffuse intensity, including the dynamic of the whole molecule, is finally adjusted by least-squares fitting.

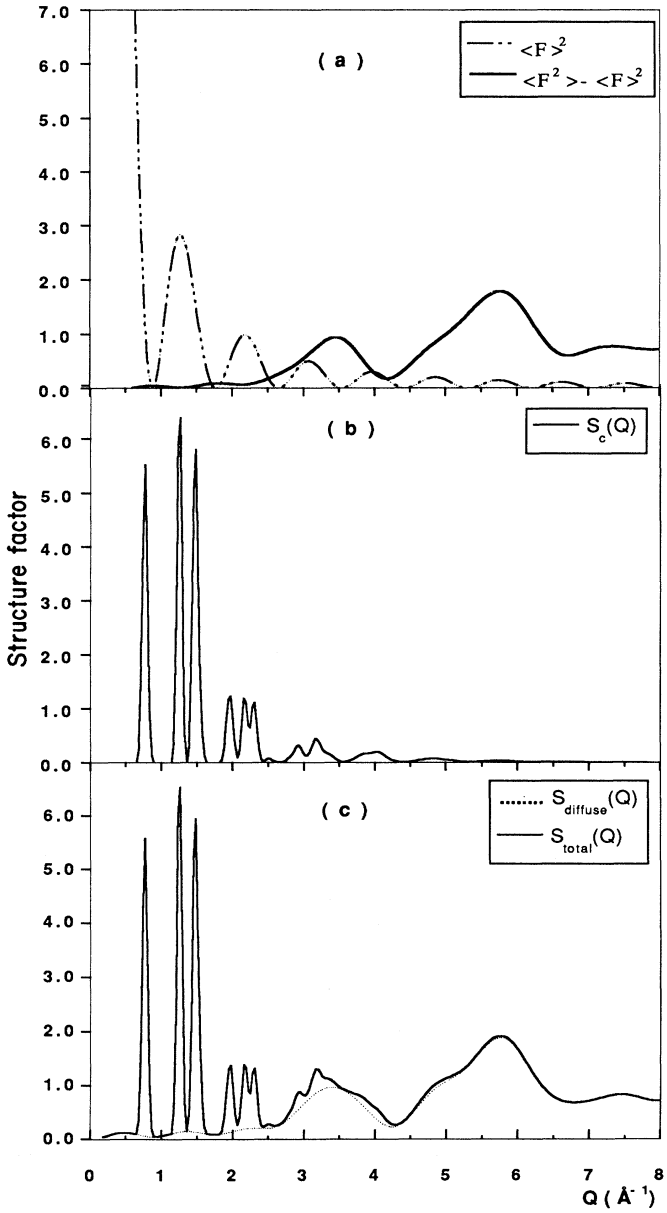

FIG. 5. Respective components of the static structure factor $S(Q)$ in the low-Q range when assuming the spherical orientational average for a powder sample. (a) Relative contributions of $\langle F\rangle^2$ and $(\Delta F)^2=\langle F^2\rangle-\langle F\rangle^2$ to the diffuse intensity. (b) Bragg scattering $S_c(Q)$. (c) Diffuse scattering $S_d(Q)$ to be compared to the total structure factor $S(Q)$.

1. Calculation of Bragg intensities

The coherent elastic scattering which is observed at each Bragg position Q_{hkl} allowed by the $Fm3m$ cubic group can be written using Eq. (18) and after powder averaging,

$$I(Q_{hkl})=C\times M_{hkl}\frac{8\pi^2}{a^3}\left[\frac{60b_c j_0(Q_{hkl}\rho)}{Q_{hkl}}\right]^2\times e^{-2WQ_{hkl}^2} \tag{19}$$

where is C a normalization constant, M_{hkl} is the multiplicity of a given Bragg reflection, a is the cell parameter of the fcc lattice[7] ($a_{295\ \mathrm{K}}=14.16$ Å), b_c is the carbon-bound coherent scattering length, and W is the Debye-Waller factor of the molecular center of mass.

In spite of a moderate instrumental resolution (the 7C2 spectrometer being not optimized for crystalline structure determination) we were able to determine the intensity of six Bragg contributions (corresponding to peaks 111, 220, [combination of 311+222], [combination of 331+420], 422, 333+511), and to obtain a correct refinement of the Debye-Waller factor W from these data using Eq. (19). As a difference with Heiney *et al.*,[6] who found that the translational Debye-Waller factor of the molecular center of mass was negligible, our fit returned a weak but well-characterized value for this factor, $W=0.015(5)Q^2$.

2. Calculation of the Bragg pattern $S_c(Q)$ in the whole Q range

For the two wavelengths used, the experimental resolution is obtained as a function of Q from the analysis (assuming a Gaussian shape) of the Bragg peaks of the C_{60} pattern in the 0.5–2.5-Å^{-1} range and of the nickel powder pattern in the 2.5–10 Å^{-1} range. As an example, for $\lambda=0.7058$ Å, a polynomial adjustment of the experimental resolution gives the following:

$$\mathrm{res}(Q)=\frac{\mathrm{FWHH}}{2\ln 2}=0.0651-0.0275Q+0.015Q^2-0.00057Q^3\ . \tag{20}$$

The intensity of 115 Bragg peaks is then calculated using Eq. (19) and the result convoluted with the resolution according to

$$I_{\mathrm{Bragg}}(Q)=\sum_{h,k,l}\frac{I(Q_{hkl})}{\sqrt{\pi}\,\mathrm{res}(Q_{hkl})}\exp\left[-\frac{(Q_{hkl}-Q)^2}{\mathrm{res}(Q_{hkl})}\right]\ , \tag{21}$$

which provides a realistic diffraction pattern, reported in Fig. 5(b). It is noticeable that, due to the low diffractometer resolution, the C_{60} Bragg peaks merge into broad ripples as Q increases. This pattern, after multiplication by a calibration constant, is removed from the experimental spectrum to obtain the total diffuse scattering.

3. *Fit of the total diffuse scattering $S_d(Q)$*

Equation (14) (describing the intramolecular structure factor and inelasticity corrections) plus an additional term $B_1\langle F\rangle^2 e^{-2W}$, taking into account the fluctuations of the molecular center of mass with B_1 a normalization constant, are used to fit the total diffuse scattering spectrum in the whole Q range. In practice, 30 data points (out of 640) had to be discarded: indeed, the shape of the actual peaks of the spectrum is not exactly Gaussian which introduces errors much larger than the standard error at the position of the main Bragg peaks. The results of these fits are reported in Table I and printed in bold (fits **e** and **e''**) since we believe that they provide the most reliable values of h and p. Since the whole experimental spectrum is elucidated at high temperature, it is possible to confirm that the values of the bond lengths are remarkably independent of the choice of the Q limits. For example, it is worth noticing that the same values of h and p are found using a very limited Q-range (1.6 to 10 Å^{-1}) as fit e', Table I.

Several self-consistency checks of the various contributions to the total diffuse scattering and of the balance between diffuse and Bragg scattering terms are possible. For example, one finds for the ratio of the diffuse scattering normalization constants B/B_1 a value of 59.3 within 1% of the theoretical value of 60. In the same way, the Debye-Waller term W obtained from fluctuations of the molecular center-of-mass contribution to the diffuse scattering [Eq. (9)] is found to be equal to $W=0.0157(8)$, which compares very well to the value $W=0.015(5)$ found from the refinement of Bragg peak intensities.

Contributions of Bragg scattering $S_c(Q)$ and diffuse scattering $S_d(Q)$ to the total structure factor spectrum at 295 K in the 0–8-Å^{-1} Q range are given in Figs. 5(b) and 5(c). Figure 5(a) gives the relative contribution of the two components of the diffuse scattering as a function of Q.

In conclusion, it has been possible for the high-temperature plastic phase of the fullerene to determine with precision the respective components of $S(Q)$. Figure 6 reports the interference function $Q\times\langle F^2\rangle_{\text{dist}}$ calculated in the whole Q range; such an identification of the intramolecular structure factor in the whole range gives confidence on intramolecular bond-lengths determination.

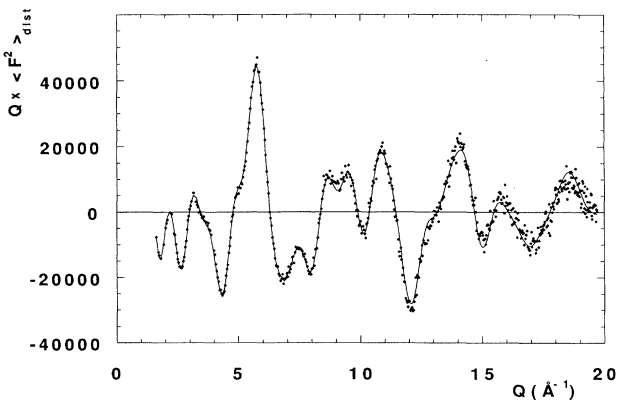

FIG. 6. Interference function $Q\langle F^2\rangle_{\text{dist}}$ in the 1.6–20-Å^{-1} range at 295 K (●, experimental data; ——, calculated values in fit **e**).

D. Determination of impurity content

The ability of fullerene powders to adsorb gases or liquids is known and we must be concerned about sample impurity content and identification. Taking advantage of the high sensitivity of our neutron-scattering technique to detect small rigid molecules, we prospected the existence of molecular oxygen, since the sample was handled in the open atmosphere, and of deuterated benzene used for washing the sample.

The test was conducted in two ways. First, the molecular form factor of oxygen and/or deuterated benzene was added to the fitting Eq. (14); the molecular parameters (distances and Debye-Waller factors) characteristic of the impurity molecule X were taken from the literature and only the normalization factor B_x was allowed to vary. So the value of the coefficient B_x gives directly the amount of the X impurity. For molecular oxygen as well as for benzene, the fits did not converge and it was thus not possible to evaluate the presence of these impurities.

Choosing a different approach, we calculated the molecular structure factor of oxygen and deuterated benzene, a few percent of which was added or removed from the experimental spectrum. The fit was then carried out using regular Eq. (14) and the value of the weighted residue was followed. The goodness of the fits was never improved for any percentage of impurity; a significant worsening was observed by adding (or removing) 1% (molar ratio) of benzene or 10% (atomic ratio) of O_2. Sensitivity to molecular oxygen was less than expected; the sensitivity should be better than 1% for objects of similar coherent cross section. In fact, the large number of C_{60} intramolecular distances ends in an amplification of the signal at the damage of the small and rigid molecule; for example, $B_{C_{60}}=b_c^2\times 60\times 59$ and $B_{O_2}=b_0^2\times 2$.

In conclusion it is only possible to assess that the impurity content in our C_{60} sample is inferior to the sensitivity of our technique, i.e., less than 3 mol of O_2 and/or 0.01 mole of C_6H_6 per fullerene mole.

VI. DISCUSSION

The geometry of the C_{60} molecule in solid fullerene has been determined with accuracy using neutron scattering over a large range of momentum transfer values, giving one more proof, if needed, that all carbon atoms in fullerene C_{60} are equivalent within the truncated icosahedral shape. These accurate measurements have, for the first time, given access to the temperature dependence of the bond lengths h and p in the solid state.

It seems important to discuss at which level of confidence the results summarized in Table I should be taken. A first comment from the inspection of the residue of the fits is that the statistical precision reached using this spectrometer was good and that all types of

corrections have been correctly met. More fundamentally, the covariance matrix (see Table II and Sec. V B) shows that such a high level of accuracy on bond lengths is reached because the two distances, h and p, are almost completely uncorrelated with the other parameters. This unusual behavior is explained as follows: the determination of each intramolecular distance in a molecule without special symmetry is defined by a single sine function of argument Qr_{ij}. Since the many distances and corresponding sine functions in the fullerene C_{60} are related to h and p, these two parameters are defined with a high degree of redundancy, the observed pattern being a fingerprint which determines unambiguously and precisely the molecule. A bad evaluation of any other parameter which does not participate to the interference of the 23 normalized sine functions does not affect the resolution obtained on the two lengths. On an absolute scale, the measured lengths are also limited to a precision of about one part per thousand due to the uncertainty of the wavelength calibration.

The validity of the truncated icosahedral model for the C_{60} molecule is accurately verified by the quality of the fits. Indeed, the residue is almost that expected by the statistical uncertainty and there is no marked structure of the residue as a function of Q. There would be no way to obtain a good fit if the reduction of free parameters from 1776 to 10 was not fully valid. We build several simulated spectra of the distorted C_{60} molecule with a statistical noise as in the experimental data. For example, oblate or prolate distortions of one part per thousand in the sphere diameter increases significantly the residue. That is consistent with a precision of 0.001 Å for h and p. Other types of distortion of the icosahedral group symmetry are currently under investigation.

The fitting procedure with a reduced number of parameters being validated, this type of experiment and data treatment could easily be extended for example to a C_{60} molecule enclosing a metallic ion (only two extra parameters). Determination of the Debye-Waller factor of the metal-carbon distance would be of special interest. The study of substituted C_{60} would certainly be more difficult but possible. Substitution could be accompanied by a distortion of the sphere and a multiplicity of C—C bond lengths; in such case the number of parameters would increase dramatically, but continuous function for the distortion may be thought of.

Finally, it is worth underlining that the C_{60} fullerene is the best system which might be dreamed of for modeling orientational disorder in molecular crystals. The room-temperature diffraction pattern may be completely described since, in this case, spherical orientational average and negligible intermolecular correlations lead to a simplified form of the static structure factor. It would be of interest to follow, with the same approach, the carbon atom localization and the freezing of reorientational motion as the temperature decreases.

ACKNOWLEDGMENTS

The Lasir is "l'Unité Propre de Recherche No. 2631 du CNRS." The Laboratoire Léon Brillouin is "l'Unité Mixte de Recherche No. 12 du CNRS" et du Commissariat á l'Energie Atomique." The Laboratoire de Chimie de l'Ecole Normale Supérieure is "l'Unité de Recherche Associée au CNRS No. 1110."

[1]W. Krätschmer, K. Fostiropoulos, and D. R. Huffman, Chem. Phys. Lett. **170**, 167 (1990).

[2]C. Coulombeau and A. Rassat, J. Chim. Phys. Phys. Chim. Biol. **84**, 875 (1987).

[3]C. S. Yannoni, R. D. Johnson, G. Meijer, D. S. Bethune, and J. R. Salem, J. Phys. Chem. **95**, 9 (1991).

[4]K. Hedberg, L. Hedberg, D. S. Bethune, C. A. Brown, H. C. Dorn, R. D. Johnson, and M. de Vries, Science **254**, 410 (1991).

[5]J. M. Hawkins, A. Meyer, T. A. Lewis, S. Loren, and F. J. Hollander, Science **252**, 312 (1991).

[6]P. A. Heiney, J. E. Fischer, A. R. McGhie, W. J. Romanow, A. M. Denenstein, J. P. McCauley, A. B. Smith III, and D. Cox, Phys. Rev. Lett. **66**, 2911 (1991); R. Sachidanandam and A. B. Harris, *ibid.* **67**, 1467 (1991).

[7]W. I. F. David, R. M. Ibberson, J. C. Matthewman, K. Prassides, T. S. J. Dennis, J. P. Hare, H. W. Kroto, R. Taylor, and D. M. R. Walton, Nature **353**, 147, (1991); W. I. F. David, R. M. Ibberson, T. S. J. Dennis, J. P. Hare, and K. Prassides, Europhys. Lett. **18**, 219 (1992).

[8]H. B. Bürgi, E. Blanc, D. Schwarzenbach, S. Liu, Y. Lu, M. K. Kappes, and J. A. Ibers, Angew. Chem. Int. Ed. Engl. **31**, 5 (1992); **31**, 641 (1992).

[9]F. Li, D. Ramage, J. S. Lannin, and J. Conceicao, Phys. Rev. B **44**, 13 167 (1991).

[10]A. K. Soper, W. I. F. David, D. S. Sivia, T. J. S. Dennis, J. P. Hare, and K. Prassides, J. Phys. Condens. Matter **4**, 6087 (1992).

[11]C. S. Yannoni, P. P. Bernier, D. S. Bethune, G. Meijer, and J. R. Salem, J. Am. Chem. Soc. **113**, 3190 (1991).

[12]A. D. J. Haymet, Chem. Phys. Lett. **122**, 421 (1985).

[13]M. Haeser, J. Almlöf, and G. E. Scuseria, Chem. Phys. Lett. **181**, 497 (1991).

[14]N. W. Ashcroft, Europhys. Lett. **16**, 355 (1991).

[15]P. A. Egelstaff, in *Methods of Experimental Physics, Vol. 23, Neutron Scattering* (Academic, London, 1987), p. 405.

[16]M. C. Bellissent-Funel, L. Bosio and J. Teixeira, J. Phys. Condens. Matter **3**, 4065 (1991).

[17]P. Damay, F. Leclercq, and P. Chieux, Phys. Rev. B **41**, 9676 (1990).

[18]R. E. Haufler, J. Conceicao, L. P. Chibante, Y. Chai, N. E. Byrne, S. Flanagan, M. M. Haley, S. C. O'Brien, S. C. Pan, Z. Xiao, W. E. Billups, M. A. Ciufolini, R. H. Hauge, J. L. Margrave, L. J. Wilson, R. F. Curl, and R. E. Smalley, J. Phys. Chem. **94**, 8634 (1990).

[19]P. M. Allemand, A. Koch, F. Wudl, Y. Rubin, F. Diederich, M. M. Alvarez, S. J. Anz, and R. L. Whetten, J. Am. Chem. Soc. **113**, 1050 (1991).

[20]M. C. Bellissent-Funel, P. Chieux, D. Levesque, and J. J. Weiss, Phys. Rev. A **39**, 6310 (1989).

[21]G. Dolling, B. M. Powell, and V. F. Sears, Mol. Phys. **37**, 1859 (1979).

[22]G. Placzek, Phys. Rev. **86**, 377 (1952).

[23]In the present analysis, the average intramolecular distances r_{ij} are defined without any reference to crystallographic axes, as in the case of liquid structure analysis. It is important to underline this point since in crystal structure refinement, the rigid body motion of molecules leads to corrections to the intramolecular interatomic distances [for example, angular oscillations can cause atomic positions to be displaced towards the center of rotation—see, for example, D. W. J. Cruickshank, Acta Crystallogr. **14**, 896 (1961)].

[24]G. Walford, J. H. Clarke, and J. C. Dore, Mol. Phys. **33**, 25 (1977).

[25]The fit procedure is based on the gradient method, using analytical derivatives of the function with respect to each parameter. A special subroutine, "C_{60} distances," called at each iteration, calculates the 23 intramolecular distances r_{ij} as a function of h and p as well as the derivatives dr_{ij}/dh and dr_{ij}/dp. The derivatives are also used to evaluate the Debye-Waller factor according to Eq. (15). The program source may be sent on request.

[26]L. Pauling, *The Nature of the Chemical Bond and the Structure of Molecules and Crystals,* 3rd ed. (Cornell University Press, Ithaca, N.Y., 1960).